J Mater Sci (2006) 41:5994–6000
DOI 10.1007/s10853-006-0498-5

Effects of nitrogen content and weld cooling time on the simulated heat-affected zone toughness in a Ti-containing steel

Kook-soo Bang · Chan Park · Stephen Liu

Received: 25 May 2004 / Accepted: 18 August 2005 / Published online: 1 August 2006

Abstract An increase of nitrogen content in a 0.02 wt% Ti-containing carbon-manganese steel resulted in a low coarsening rate of TiN particles in the heat-affected zone (HAZ), which led to an accelerated ferrite transformation instead of ferrite side plates during weld cooling cycle. The mixed microstructure of ferrite side plate, acicular ferrite and grain boundary polygonal ferrite in the simulated HAZ produced higher toughness. However, the increase of nitrogen content gradually increased the free nitrogen content in the HAZ and deteriorated HAZ toughness. Impact energy of the simulated HAZ (with $\Delta t_{8/5}$ ~60 s) at –20 °C deteriorated by about 97 J per 0.001 wt% free nitrogen, in the free nitrogen range from 0.0009 wt% to 0.0034 wt%, even though the HAZ has the tough mixed microstructure. Cooling time after welding influenced the HAZ microstructure and toughness as well, and maximum toughness was obtained when cooling produced the tough mixed microstructure. Therefore, for a high HAZ toughness, both nitrogen content and cooling time should be controlled to obtain the tough mixed microstructure and to keep the free nitrogen content low. The optimal nitrogen content and cooling time from 800 °C to 500 °C were 0.006 wt% and between 60 s and 100 s, respectively, in this experiment.

K. Bang (✉) · C. Park
Division of Advanced Materials Science and Engineering,
Pukyong National University, Pusan 608-739, Korea
e-mail: ksbang@pknu.ac.kr

C. Park
e-mail: chanpark@pknu.ac.kr

S. Liu
Center for Welding, Joining and Coatings Research,
Colorado School of Mines, Golden, CO 80401, USA
e-mail: sliu@mines.edu

Introduction

Extensive studies have shown that titanium addition to steel is one of the most effective methods of improving the heat-affected zone (HAZ) toughness of the steel. Fine TiN particles prevent the coarsening of austenite grains in the HAZ and act as heterogeneous nucleation sites for the ferrite transformation during the weld cooling cycle, thereby resulting in a fine microstructure [1–6]. To obtain a uniform distribution of fine TiN particles, the steel processing and chemistry (titanium and nitrogen contents) must be adequately controlled. Kasamatsu et al. [7] investigated the effect of titanium and nitrogen contents on the size and distribution of TiN particles and showed that the number of the particles increases with an increase of nitrogen content. Watanabe et al. [8] reported that TiN precipitated profusely when the nitrogen content of a Ti-containing steel was increased above 0.004 wt% and when the rolling process was strictly controlled.

In general, steels with high nitrogen content are expected to have low HAZ toughness due to the presence of 'free' nitrogen in solid solution. Hannerz [9] reported an increase of 2–4 °C in ductile-brittle transition temperature per 10 ppm increase in nitrogen in the HAZ of carbon-manganese steels. Cuddy et al. [10] showed that steels containing titanium and nitrogen in excess of 0.02 wt% and 0.007 wt%, respectively,

had poor HAZ toughness independent of the microstructure. Thus, even in Ti-containing steels, they suggested that nitrogen levels must be kept low. Bang and Jeong [11] also showed that the amount of TiN increased with an increase of nitrogen content. However, if the nitrogen content increased above 0.01 wt%, the detrimental effect of free nitrogen on the HAZ toughness would be greater than the beneficial effect caused by the stable TiN particles. Some other results, however, are contradictory. Zajac et al. [12] showed that high nitrogen steel (0.013 wt% N) has a higher HAZ toughness than low nitrogen steel (0.003 wt% N) if microalloying elements such as titanium and vanadium are carefully balanced in the composition and when the welding parameters are selected adequately. They showed that excellent HAZ toughness was obtained for high nitrogen Ti-V steel when the cooling time between 800 °C and 500 °C ($\Delta t_{8/5}$) was shorter than 30 s. However, a sharp rise of impact transition temperature (ITT) in this steel was observed when $\Delta t_{8/5}$ was longer than 30 s. This result was confirmed by Liao et al. [13]. From all these previous results, it is clear that the effect of nitrogen on the HAZ toughness of Ti-containing steels is very complex depending on both welding parameters and microalloying elements.

This paper examines the effects of both nitrogen content and weld cooling time on the simulated HAZ toughness of Ti-containing carbon-manganese steel. The steel was manufactured by thermomechanical controlled processing (TMCP). Changes in simulated HAZ toughness were interpreted in terms of both the microstructure and amount of free nitrogen. The presence of free nitrogen in the HAZ was confirmed by internal friction measurement and the amount was measured using the hydrogen hot extraction analysis.

Materials and experimental procedures

Five 0.14 wt% C-1.5 wt% Mn steels were melted using a vacuum induction furnace with constant titanium content of 0.02 wt%. Nitrogen content was varied in the range of 0.0006–0.016 wt%. After soaking the ingot at 900 °C for one hour, it was thermomechanically controlled to the final thickness of 12.5 mm. The finish-rolling temperature was 760 °C and the subsequent accelerated cooling rate was 10 °C s^{-1}. The steel exhibited a very fine ferritic-pearlitic microstructure with a small amount of bainite. Ferrite grain size was about 5 μm. The final chemical compositions and mechanical properties of the plates are presented in Table 1. The precipitates in the base plates and simulated HAZs were observed using carbon extraction replicas and a scanning transmission electron microscope (JEOL 2000CX STEM) operating at 200 kV. Specimens for HAZ simulation measuring 10.2 × 10.2 × 55 mm were subject to weld thermal cycles using a weld thermal cycle simulator (Thermorestor W). The heating rate was 135 °C s^{-1} to the 1350 °C peak temperature. The cooling rates were selected to give $\Delta t_{8/5}$ values from 10 s to 150 s. These temperature-time cycles simulated the thermal experience of the material near the fusion boundary of a 25 mm plate when welded with heat input from 1.8 kJ mm^{-1} to 11.5 kJ mm^{-1}. After thermal cycling, standard 2 mm V-notch Charpy impact test specimens were machined and tested at –20 °C.

Internal friction measurement was carried out to investigate the presence of free nitrogen in the HAZ. Steel E (see Table 1) was gas metal arc (GMA) welded with 4 kJ mm^{-1} heat input and the specimen was obtained from the HAZ near the fusion boundary in the form of a sheet of 1 × 5 × 110 mm. Care was taken to avoid deformation and heating during specimen preparation. The measurement was conducted using a torsion pendulum type apparatus (Sinkuriko IFM 1500-M) in the temperature range of –30–110 °C with a pendulum frequency of 2.3 Hz. For the quantitative measurement of free nitrogen, hydrogen hot extraction analysis was carried out. Two grams of needle shape millings from the simulated HAZ ($\Delta t_{8/5}$ ~ 60 s) were placed in a combustion boat and introduced into a tube furnace set at 450 °C, with an argon flow of 0.3 l min^{-1}. Gas flow was then switched to hydrogen at 0.3 l min^{-1}. After four hours, the gas flow was changed back to argon and the sample was allowed to cool down in the furnace. The nitrogen contents of the samples before and after exposure to the hydrogen atmosphere were

Table 1 Chemical composition and mechanical properties of steels used

Steels	Chemical composition (wt%)								Mechanical properties				
	C	Si	Mn	P	S	Al	Ti	N	TS (MPa)	YS (MPa)	El (%)	H_V (1 kg)	$_vE$–20 (J)
A	0.13	0.11	1.53	0.01	0.005	0.04	0.02	0.0006	641	372	13	177	337
B	0.14	0.11	1.58	0.01	0.004	0.04	0.02	0.006	594	460	13	180	205
C	0.14	0.10	1.51	0.01	0.005	0.05	0.02	0.011	576	493	13	179	176
D	0.14	0.11	1.53	0.01	0.005	0.05	0.02	0.013	573	461	14	183	203
E	0.15	0.10	1.56	0.01	0.005	0.04	0.02	0.016	591	509	12	195	227

then measured by the inert gas fusion process (LECO TC-436). The free nitrogen value was given by the difference between them [14].

Results and discussion

To study the effect of nitrogen content on TiN precipitates, carbon extraction replicas were used to observe particle size distributions in the base plate and the simulated HAZ ($\Delta t_{8/5}$ ~ 60 s) of two steels with different nitrogen content, Steels B (0.006 wt% N) and E (0.016 wt% N). The number of particles in the size range of less than 5 nm to 100 nm was counted at 5 nm class intervals within an area of approximately 8.4 μm^2. Typical TEM micrographs are shown in Fig. 1. The mean particle size and number density of the particles are presented in Table 2, indicating little differences between the two base plates. The mean particle size found in Steels B and E are 7.2 and 8.4 nm, respectively. The corresponding number densities of the precipitates are 2.1×10^8 and 1.7×10^8 mm^{-2}, respectively. However, significant differences were shown in the HAZ with 16.8 nm and 10.3 nm mean particle size, and 0.3×10^8 mm^{-2} and 1.1×10^8 mm^{-2} number density, respectively. Compared to those in the base plate, the particles in the HAZ of both steels were coarser. However, the degree of coarsening in the two HAZ's was different, with less coarsening in Steel E that had higher nitrogen content.

Table 2 Mean particle size and number density of TiN particles in the base plate and HAZ of steels B and E

Steels	Mean particle size (nm)*		Number density (/mm^2)	
	Base plate	HAZ	Base plate	HAZ
B	7.2	16.8	2.1×10^8	0.3×10^8
E	8.4	10.3	1.7×10^8	1.1×10^8

*The shortest edge length in cuboid

In general, a larger volume fraction of fine particles will result in more effective grain growth inhibition, thus Steel E is expected to have smaller austenite grain size, which will accelerate phase transformations in the HAZ during weld cooling cycle. Indeed this effect of high nitrogen content was reported in other experiments. Zajac et al. [12] showed that the austenite grain size is about three times smaller in high nitrogen steel (0.013 wt% N) than in steel with 0.003 wt% N, despite similar manufacturing process and level of titanium and vanadium. Continuous cooling transformation (CCT) diagrams of Steels B and E were constructed and compared to study the effect of nitrogen content on HAZ phase transformations. After austenitizing at 1350 °C for 5 s, the hollow cylindrical shaped specimens were cooled with various cooling rates to obtain dilatation curves. Figure 2 shows CCT diagrams of both steels. As expected, the transformation curves of high nitrogen steel (Steel E) are shifted to shorter

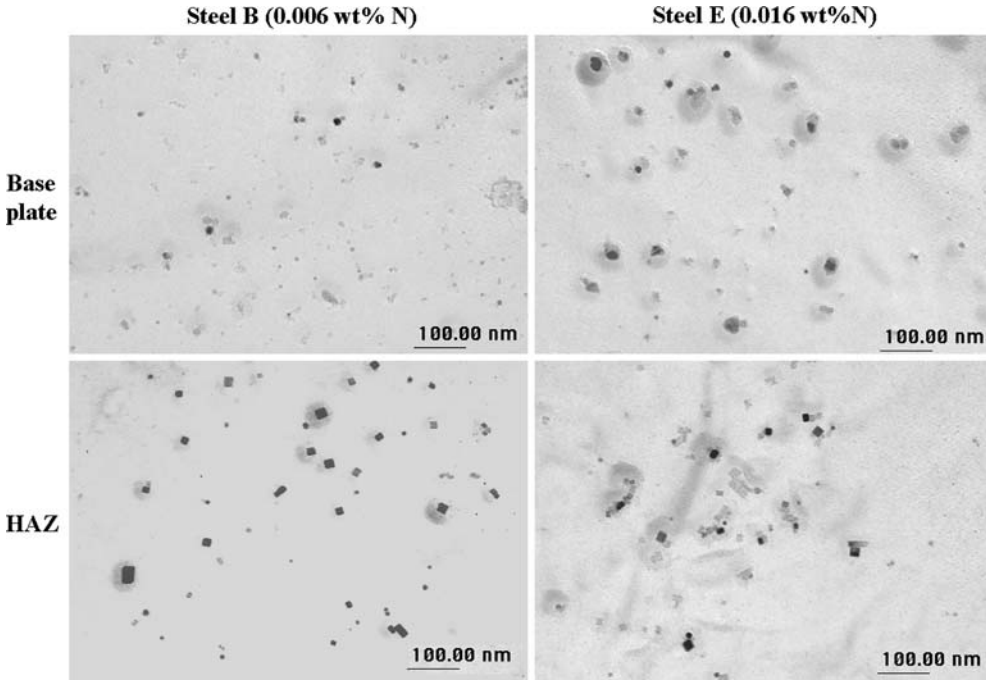

Fig. 1 Typical TEM micrographs of carbon extraction replicas from Steels B and E ($\Delta t_{8/5}$ is 60 s for HAZ)

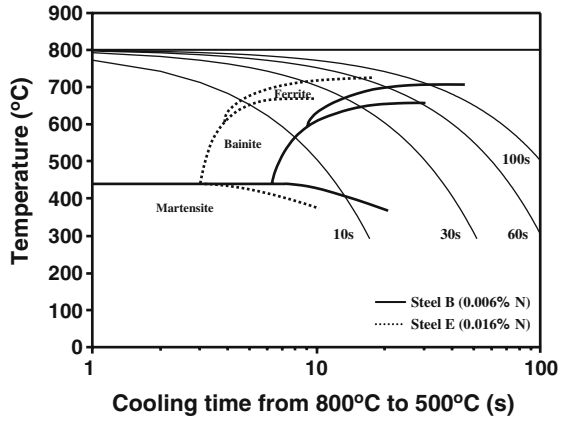

Fig. 2 CCT diagrams of Steels B and E. Solid line: Steel B, broken line: Steel E

times, indicating accelerated phase transformations in the HAZ. The observed low coarsening rate of TiN particles in Steel E can readily be explained using the Wagner equation. Under the condition of diffusion control, the rate of change of the particle radius, dr/dt, is directly related to the concentration of the rate-limiting species. The Wagner equation is given as: [15]

$$r^3 - r_0^3 = 8D\gamma\Omega Xt/9RT$$

where D is the diffusion coefficient of the rate-limiting species, γ the interfacial energy between the matrix and particle, Ω the molar volume and X the concentration of the rate-limiting species. R is the universal gas constant and T is the temperature. In the case of TiN particles, the relevant solutes are titanium and nitrogen. As the diffusion coefficient of titanium is many orders of magnitude lower than that of nitrogen, titanium is the rate-limiting species. Using the solubility product of TiN given below, [16]

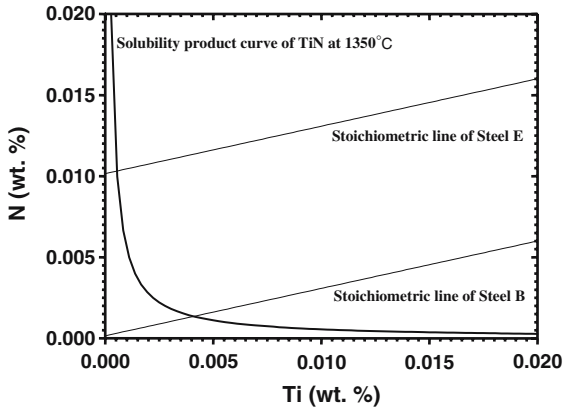

Fig. 3 Solubility diagram for titanium nitride, showing the effect of nitrogen content in the steel on the soluble titanium content in the HAZ at 1350 °C

$$\log[\mathrm{Ti}][\mathrm{N}] = -16192/T + 4.72$$

the concentration of soluble titanium in the HAZ can be calculated. Figure 3 shows the solubility product curve at 1350 °C peak temperature. The stoichiometric lines of TiN in Steels B and E, which pass through the composition of each steel, are also shown in the figure. At equilibrium, the intersection between the solubility product curve and the stoichiometric line will indicate the soluble titanium and nitrogen content in the HAZ at 1350 °C. From the figure, the soluble titanium content is about 0.0005 wt% for Steel E, much lower than the 0.0041 wt% for Steel B. Therefore, an increase of nitrogen content in steel results in low soluble titanium concentration and low coarsening rate of TiN particles, thus accelerating austenite decomposition in the HAZ.

The impact toughness of simulated HAZ of the steels is given in Table 3. $\Delta t_{8/5}$ is constant at 60 s. The table also contains nitrogen content in the base plate and free nitrogen content in the HAZ, which is discussed later. Figure 4 shows the variation of the simulated HAZ impact absorbed energy with nitrogen content in the base plate. After an initial low value of 48 J for 0.0006 wt% N, impact toughness value increased up to 270 J at 0.006 wt% N, and then decreased to 24 J at 0.016 wt% N. The optical microstructures in each HAZ were classified according to schemes proposed in the literature [17]. Table 4 shows the measured volume fraction of microstructural constituents in each HAZ. While ferrite side plates (i.e., upper bainite and Widmanstätten ferrite) are dominant in Steel A, a mixed microstructure of ferrite side plates (SP), acicular ferrite (AF) and grain boundary or polygonal ferrite (F) is observed in all other steels. As example, Figure 5 shows typical HAZ optical micrographs of Steels A and B. Each microstructural constituent is identified in the Fig. (5B). Even though all HAZ's, except Steel A, have the same type of mixed microstructure, the volume fractions of each microstructural constituent in these simulated HAZ's are different. The volume fraction of grain boundary polygonal ferrite (F) increased with an increase of nitrogen content, 43% in Steel E and 12% in Steel B. This difference supports the observation of the effect of nitrogen on the acceleration of ferrite transformation in the HAZ discussed above. As Steel A has low nitrogen content (0.0006 wt%), it shows a microstructure predominated by ferrite side plate and a low HAZ toughness. In contrast, Steel B with its higher nitrogen content (0.006 wt%) shows a mixed microstructure and a high HAZ toughness. Comparison of SEM micrographs of Steels A and B in Fig. 6 shows that the

Table 3 Impact toughness of simulated HAZ of the steels at –20 °C ($\Delta t_{8/5}$ = 60 s)

Steels	Nitrogen content in base plate (wt%)	Free nitrogen content in HAZ (wt%)	Impact absorbed energy (J)
A	0.0006	0.0001	36.9, 39.7, 68.0 (48.2)*
B	0.006	0.0009	199, 291.1, 319.5 (269.9)
C	0.011	0.0029	120.2, 70.1, 41.3 (77.2)
D	0.013	0.0034	21.2, 36.5, 19 (25.6)
E	0.016	0.0050	20.5, 25.3, 27.2 (24.3)

*Average values are given in parenthesis

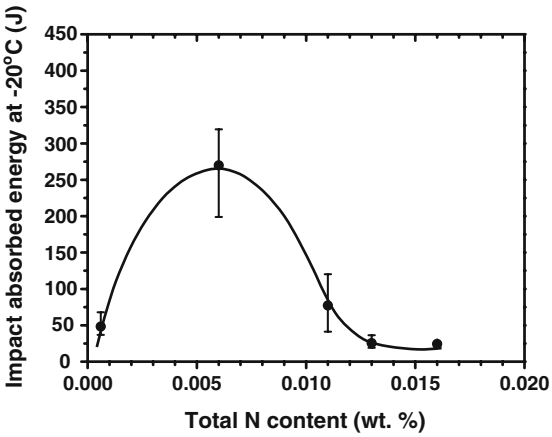

Fig. 4 HAZ impact absorbed energy at –20 °C as a function of nitrogen content in steel ($\Delta t_{8/5}$ ~ 60 s)

improvement of the HAZ toughness in Steel B can be attributed to fine AF. However, even though Steels C, D, and E have the same type of mixed microstructure as Steel B, their HAZ toughness is very low, clearly indicating that nitrogen content plays an important role even if HAZ has tough mixed microstructures.

To study the reason why Steels C, D, and E have low HAZ toughness, the presence of free nitrogen in the HAZ was investigated both qualitatively and quantitatively. Free nitrogen can exist in the HAZ when nitrogen is in excess of that required for stoichiometry with titanium. Free nitrogen can also exist by the dissolution of nitrides during the weld thermal cycle. In this study, the presence of free nitrogen in the HAZ was confirmed first by the internal friction measurement. Examining GMA ferritic weld metal using the internal friction method, den Ouden [18] showed that the internal friction spectrum could be separated into two normal Snoek peaks and four additional peaks due to the presence of Mn. In this study, internal friction of HAZ was measured using specimens obtained from the HAZ of GMA welded Steel E. Data interpretation followed den Ouden's procedure. The measured internal friction curve was separated into five different peaks, after subtracting the background, as shown in Fig. 7. The N2 and C peaks with internal friction of 3.89×10^{-4} and 0.18×10^{-4}, respectively, are normal peaks of nitrogen and carbon, and N1, N3 and N4 peaks with internal friction of 1.60×10^{-4}, 1.69×10^{-4} and 0.34×10^{-4}, respectively, are extra peaks of nitrogen due to the presence of manganese. The N2 peak

Table 4 Volume fraction of microstructural constituents in simulated HAZ of the steels ($\Delta t_{8/5}$ = 60 s)

Steels	F*	AF*	SP*	P*
A	0	16	84	0
B	12	34	47	7
C	19	26	47	8
D	26	26	37	11
E	43	19	20	18

*F, AF, SP and P means grain boundary or polygonal ferrite, acicular ferrite, ferrite side plates and pearlite, respectively

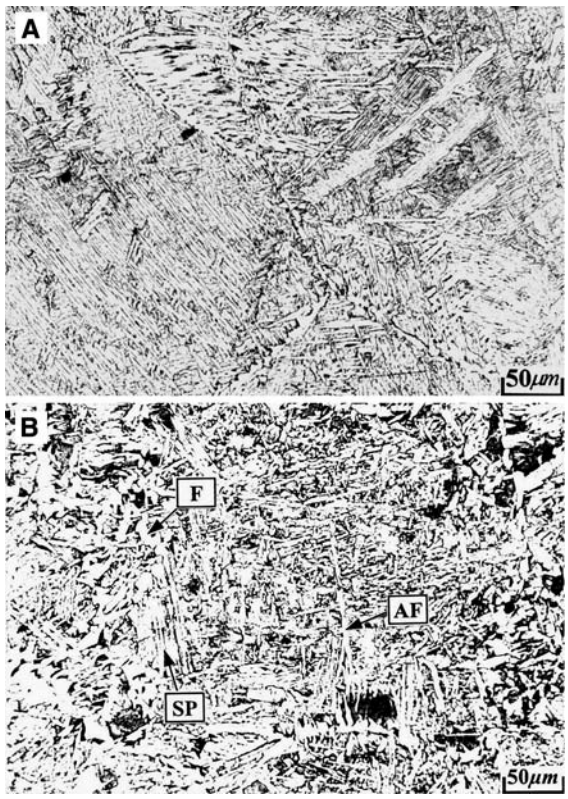

Fig. 5 Typical microstructures of (**a**) Steel A and (**b**) Steel B. The various microstructural constituents indicated in the figure are defined in the text

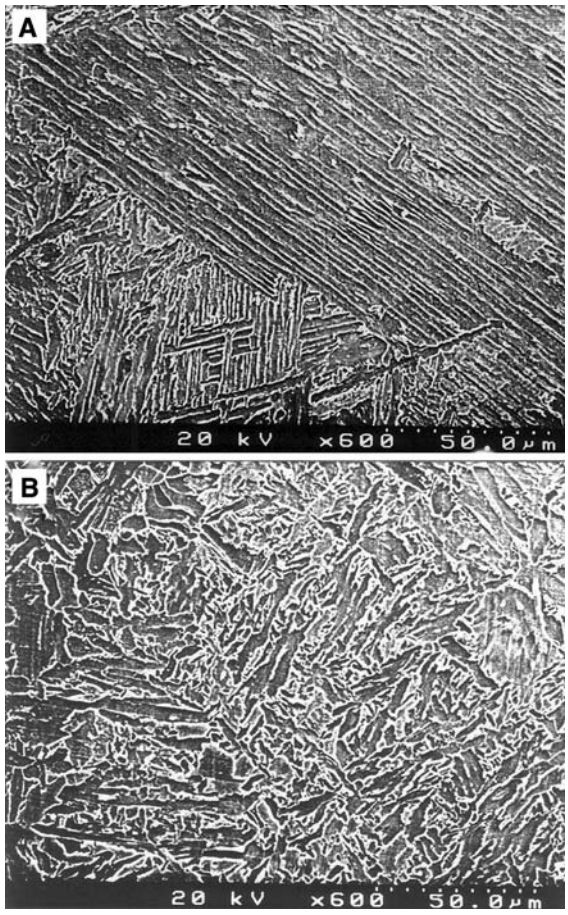

Fig. 6 Typical SEM micrographs of (**a**) Steel A and (**b**) Steel B

corresponding to nitrogen is most prominent in the HAZ of Steel E.

Hydrogen hot extraction analysis determined quantitatively the free nitrogen content in the HAZ of each steel. After simulating the weld thermal cycle of $\Delta t_{8/5}$ ~ 60 s, samples were prepared and analyzed following the procedure mentioned before. The measured contents in Table 3 increased gradually with increasing nitrogen content in the base plate. Steel E with the highest nitrogen content (0.016 wt%) in this series of experiments showed about 0.005 wt%, which is about 30% of the added content. From this result, the low HAZ toughness of Steels C, D, and E can be attributed to their larger amounts of free nitrogen. To differentiate the effect of free nitrogen on the HAZ toughness from the effect of microstructure, the impact-absorbed energies of Steels B, C, and D were compared. The impact toughness data of Steel E was excluded in the comparison because its volume fractions of microstructural constituents are quite different from those observed in the others, e.g. 43% of grain boundary polygonal ferrite (F) as compared with 12, 19, and 26% in Steels B, C, and D. As shown in Fig. 8, impact toughness decreased linearly with increasing free nitrogen; Steel B with 0.0009 wt% free nitrogen had 270 J while Steel D with 0.0034 wt% had only 26 J. The slope of the line in the figure indicates that the HAZ impact absorbed energy at –20 °C with the mixed microstructure decreased by about 97 J per 0.001 wt% free nitrogen.

The effect of cooling time on the HAZ toughness was studied using Steel B. Table 5 shows the impact toughness of simulated HAZ when $\Delta t_{8/5}$ was varied from 10 s to 200 s. Impact toughness increased gradually with increasing cooling time but exhibited a maximum value of 320 J at 100 s. Optical microstructure observation showed only upper bainite at 10 s, a mixed microstructure of SP, AF and fine F at 60 and 100 s, and a mostly coarse F at 150 and 200 s. These results matched well with the CCT diagram shown in Fig. 2. Therefore, it is clear that both nitrogen content and

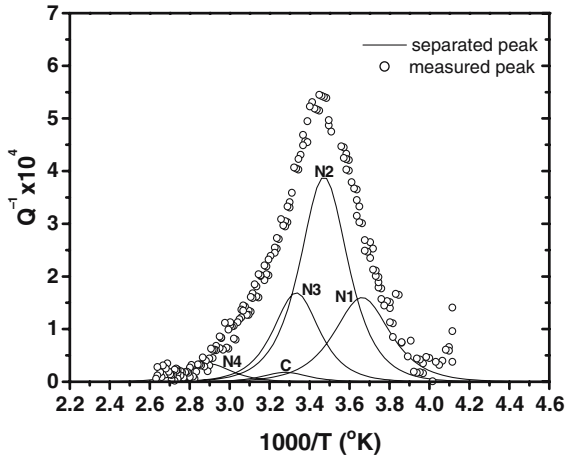

Fig. 7 Separation of measured internal friction curve of HAZ of Steel E into its component peaks. Dot: measured peak, solid lines: separated peaks

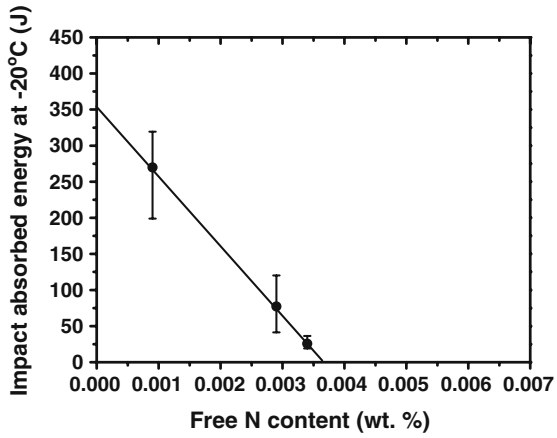

Fig. 8 HAZ impact absorbed energy at –20 °C as a function of free nitrogen content in HAZ ($\Delta t_{8/5}$ ~ 60 s)

Table 5 Impact toughness of simulated HAZ of steel B at –20 °C

$\Delta t_{8/5}$(s)	Impact absorbed energy (J)
10	62.8, 20.8, 71.4 (51.7)*
30	209.5, 211.5, 210.5 (210.5)
60	199, 291.1, 319.5 (269.9)
100	383.6, 222.6, 354.7 (320.3)
150	175.6, 210, 145.1 (176.9)
200	181.9, 223.1, 255.9 (220.3)

*Average values are given in parenthesis

weld cooling time should be controlled to obtain the mixed microstructure for high HAZ toughness. If nitrogen content is too low and/or the cooling time is too short, ferrite side plate dominant microstructure is obtained and toughness is low. On the other hand, if nitrogen content is too high and/or the cooling time is too long, coarse grain boundary polygonal ferrite is obtained and toughness is deteriorated. This transformation behavior explains why the high nitrogen steel (0.013 wt% N) has a lower impact transition temperature than low nitrogen steel (0.003 wt% N) for $\Delta t_{8/5}$ shorter than 30 s [12]. In this experiment, maximum toughness was obtained for the mixed microstructure of SP, AF and fine F when nitrogen content is 0.006 wt% and $\Delta t_{8/5}$ is 60–100 s. As nitrogen influences the HAZ toughness because of the presence of free nitrogen, nitrogen content should be kept low even if the desirable tough mixed microstructure is obtained. The optimal content of 0.006 wt% nitrogen in this experiment is in fact close to that required for stoichiometric combination with the titanium content of 0.02 wt%.

Conclusions

The effects of nitrogen content and weld cooling time on the simulated HAZ toughness of Ti-containing carbon–manganese steel were investigated and interpreted in terms of both microstructure and amount of free nitrogen present. The main results obtained are as follows.

(1) An increase of nitrogen content resulted in a low coarsening rate of TiN particles in the HAZ due to the low concentration of soluble titanium. This caused an acceleration of ferrite transformation instead of ferrite side plate in the HAZ. Higher HAZ toughness was obtained in the mixed microstructure of ferrite side plate, acicular ferrite and grain boundary polygonal ferrite.

(2) An increase of nitrogen content increased the free nitrogen content in the HAZ and deteriorated HAZ toughness despite the optimal mixed microstructure. Impact absorbed energy of the simulated HAZ ($\Delta t_{8/5} \sim 60$ s) at –20 °C decreased by about 97 J per 0.001 wt% free nitrogen in the free nitrogen range from 0.0009 wt% to 0.0034 wt%.

(3) Cooling time after welding also influenced the simulated HAZ microstructure and toughness, and maximum toughness resulted at the cooling rate to form the optimal mixed microstructure. Therefore, for a high HAZ toughness, both nitrogen content and cooling time should be controlled to obtain the mixed microstructure as well as low free nitrogen content. The optimum conditions for 0.02 wt% titanium content were 0.006 wt% nitrogen and 60–100 s $\Delta t_{8/5}$.

Acknowledgements One of the authors (K.-s. Bang) wishes to acknowledge the financial support from POSCO, Pohang, Korea and would also like to thank B.-c. Kim for his contributions to this research.

References

1. Wang G, Lau T, Weatherly G, North T (1989) Metall Trans 20A:2093
2. George T, Kennon N (1972) J Austral Inst Met 17:73
3. Maurickx T, Taillard R (1989) In: Proceedings of the Conference on High Nitrogen Steels, Lille, May 1989, J Foct, A Hendry (eds) Institute of Metals, p 327
4. Edwards R, Squires I, Barbaro F (1986) Austral Weld J Autumn 11
5. Cuddy L, Raley J (1983) Metall Trans 14A:1989
6. Loberg B, Nordgren A, Stride J, Easterling K (1984) Metall Trans 15A:33
7. Kasamatsu Y, Takashima S, Hosoya T (1979) J Iron Steel Inst Jpn 65:1232
8. Watanabe I, Suzuke M, Yamazaki Y, Tokunaga T (1982) J Jpn Weld Soc 51:118
9. Hannerz N (1978) In: Proceedings of the Conference on Welding of HSLA (microalloyed) Structural Steels, Rome, November 1977, A Rothwell, J. Malcolm Gray (eds) ASM, p 365
10. Cuddy L, Raley J, Poter L (1984) In: Proceedings of the Conference on HSLA Steels Technology and Applications, Philadelphia, October 1983, M Korchynsky (eds) ASM, p 697
11. Bang K-s, Jeong H-s (2002) Mater Sci Technol 18:649
12. Zajac S, Siwecki T, Svensson L-E (1988) In: Proceedings of the Conference on HSLA Steels, Pittsburgh, November 1987, AJ DeArdo Jr (ed) TMS, p 511
13. Liao F, Liu S, Olson D (1994) In: Proceedings of International Conference OMAE 93, Gladgow, 1993, M Salama et al. (eds) ASME, p 231
14. Lau T, Sadowski M, North T, Weatherly G (1988) Mater Sci Tech 4:52
15. Wagner C (1961) Z Electrochem 65:581
16. Sawamura H, Mori T (1974) J Iron Steel Inst Jpn 60:31
17. Akselsen O, Grong Ø, Kvaale P (1986) Metall Trans 17A:1529
18. den Ouden G (1968) Brit Weld J September 436